Structural, electronic, and magnetic properties of AgnCo (n = 1–9) clusters: A first-principles study

ARTICLE *in* COMPUTATIONAL AND THEORETICAL CHEMISTRY · AUGUST 2015

Impact Factor: 1.55 · DOI: 10.1016/j.comptc.2015.05.009

2 AUTHORS:

Peter Ludwig Rodríguez-Kessler

Instituto Potosino de Investigación Científi…

5 PUBLICATIONS **2** CITATIONS

SEE PROFILE

Adán Rubén Rodríguez Domínguez

Universidad Autónoma de San Luis Potosí

25 PUBLICATIONS **18** CITATIONS

SEE PROFILE

Computational and Theoretical Chemistry 1066 (2015) 55–61

Contents lists available at ScienceDirect

Computational and Theoretical Chemistry

journal homepage: www.elsevier.com/locate/comptc

Structural, electronic, and magnetic properties of Ag_nCo (n = 1–9) clusters: A first-principles study

P.L. Rodríguez-Kessler [a,*], A.R. Rodríguez-Domínguez [b]

[a] Instituto Potosino de Investigación Científica y Tecnológica, Camino a la presa San José 2055, San Luis Potosí 78216, Mexico
[b] Instituto de Física, Universidad Autónoma de San Luis Potosí, San Luis Potosí 78000, Mexico

ARTICLE INFO

Article history:
Received 25 March 2015
Received in revised form 5 May 2015
Accepted 6 May 2015
Available online 21 May 2015

Keywords:
AgCo
Silver–cobalt
Clusters
DFT

ABSTRACT

Structural, electronic and magnetic properties of neutral Ag_nCo ($n = 1 - 9$) clusters are studied using first principles calculations based on density functional theory. For the ground state structures of the Ag_nCo clusters, the Co impurity occupies the highest coordinated position. The lowest energy structures for Ag_nCo ($n \leqslant 4$) clusters are planar, while from $n = 5$ onwards, Ag_nCo clusters showed an icosahedral growth except for Ag_9Co, which adopts an endohedral cage structure. The stability based on the binding energy showed that Ag_nCo clusters are energetically favored for the high spin configuration, however, from $n = 7$ onwards, trends to adopt the low spin or non-magnetic configurations are observed. Interestingly, in Ag_9Co the silver host quenches the magnetic moment of the encapsulated Co atom. The magnetic orderings between the impurity and the Ag_n host in Ag_nCo clusters are discussed.

1. Introduction

Transition metal clusters which are considered as possible building blocks of nanostructured materials have usually a size-dependent geometry, which clearly differ from their bulk counterparts [1,2]. Since the discovery of C_{60}, several investigations have been performed for the stabilization of cage-like structures [3,4]. It was found that when a transition metal atom is added to small clusters, there is a dramatic change in their structure and stability [5]. For example, the formation of a very symmetric silicon fullerene or a Frank–Kasper polyhedral cage structure is predicted for Ti and V doped silicon clusters with at least 12 Si atoms [6–8]. Various works with the aim of understanding of the size dependency properties of transition metal (TM) doped clusters studied in detail their stability and electronic properties using DFT calculations and in combination with experimental techniques for various elements and found encapsulated dopants in cage structures for Si_nM (M = Co, V, Cr, Fe) [9–13], Ge_nM (M = Co, Fe) [14,15], Au_nM (M = Si, Ge, Sn) [16], and Fe_nB [17], among others. Silver clusters are used principally in catalysis and optics [18,19]. Single magnetic impurities embedded on them showed a high rate stability for specific sizes suggesting the formation of closed-shell electronic structures, which was corroborated by mass spectra analysis and complementary theoretical studies [20,21]. To the best of our knowledge, experimental data about the structures of neutral Ag_nCo clusters has not been revealed so far, since the formation of neutral clusters by condensing the vapor species using inert gases is more difficult and ionization is required for mass spectrometric detection [7,9,22]. In this way, computer simulations have become a valuable tool and offer insight that may not always be possible from experiments [6]. In this work we have carried out an extensive search of the lowest-energy structures of Ag_nCo clusters (n = 1–9) by considering a number of structural isomers for each cluster size. For Ag_9Co we found an endohedral structure where the silver host quenches the local magnetic moment of the Co impurity following the 18-electron rule of delocalized valence electrons [23], which is consistent with the experimental findings of Ag_nCo^+ clusters [20]. This paper is organized as follows. Section 2 describes the theoretical methods used in this work. In Section 3, we discuss the structural and electronic properties of the clusters including the bond distances, binding energy, relative isomer energies, and the magnetic configurations. Finally, our conclusions are given in Section 4.

2. Computational details

The calculations reported in this work are based in the framework of spin-polarized density-functional theory (DFT) [24,25] within the Perdew–Burke–Ernzerhof (PBE) generalized gradient approximation (GGA) [26]. The electron–ion interactions are described using the projector-augmented wave (PAW) method

* Corresponding author.
E-mail address: peter.rodriguez@ipicyt.edu.mx (P.L. Rodríguez-Kessler).

http://dx.doi.org/10.1016/j.comptc.2015.05.009
2210-271X/

[27] implemented in the Vienna *Ab initio* Simulation Package (VASP) [28,29]. The plane wave basis set was expanded with a cut-off energy of 375 eV. For each cluster, the size of the unit cell was chosen such that the nearest distance between the neighboring images is more than 10 Å. Only the Γ point is taken into account to represent the Brillouin zone since we are dealing with isolated clusters. The atomic positions are relaxed selfconsistently without restrictions in the symmetry by the conjugated-gradient algorithm until the forces are in practice smaller than 0.005 eV/Å for all atoms [30]. The local atomic charges v_i and magnetic moments μ_i quantities have been determined following the atoms in molecules approach by using the numerical algorithm developed by Henkelman et al. [31] (see also Bader [32]). The optimal geometries have been obtained starting from graph theory by the implementation of Wang et al. [33] followed by a distance geometry optimization [34]. Two different spin configurations were taken into account in our calculations, e.g., ferromagnetic (FM) and antiferromagnetic (AFM) orderings. Depending on the number of valence electrons, (in particular d^7s^2 or d^8s^1 for Co and $d^{10}s^1$ for Ag), the values of total magnetic moment μ_T have been explored in two different spin configurations, the low spin (LS) where $\mu_T = 0$ or $1\mu_B$ and the high spin (HS) for $\mu_T = 2$ or $3\mu_B$, respectively.

3. Results

3.1. Geometric structure

The structures of Ag_nCo clusters are obtained by a single Co atom substitution on stable Ag_n structures isomers, because of it, we first discuss the results of pure silver Ag_n ($n = 2 - 10$) clusters comparing with previous reported works. The Ag_2 dimer is found to favor the singlet spin multiplicity over the triplet. The corresponding values of the bond length and binding energy are estimated to be 2.58 Å and 1.74 eV, which are found to be in good agreement with experimental data of 2.53 Å and 1.63 eV, respectively [35]. From different DFT computational methods, the reported bond lengths and energies are 2.63 Å and 1.70 eV, using a plane-wave pseudo potential method [36], 2.61 Å and 1.71 eV from a GGA method [37], among others. The stable isomer of Ag_3 is an obtuse triangle. The structures for Ag_4 to Ag_6 are structures formed by decorating the triangle with one to three atoms, resulting a planar rhombus for Ag_4, a trapezoid for Ag_5, and a D_{3h} planar triangle for Ag_6. For Ag_7 we found a D_{5h} pentagonal bipyramid (PBP). The ground state of Ag_8 is a tetra-capped tetrahedron with a T_D symmetry. Ag_9 has a C_{2v} structure over different isoenergetic isomers. For Ag_{10} a D_{2d} twinned PBP structure was obtained in the present work. In particular, the ground state structures of Ag_n clusters which have $n = 2 - 10$ are in agreement with previous DFT calculations reported by René Fournier [38]. Unlike Ag_n clusters, pure Au_n ones favor $2D$ structures for relatively large sizes. This is due to the strong relativistic effects which cause a high degree of hybridization between the *s* and *d* orbitals, however, this feature has been attributed only for gold clusters [39]. Other elements of this group such as copper and silver clusters are predicted to show $3D$ structures from $n = 7$ onwards [40].

The lowest energy structures obtained for pure Ag_n ($n = 2 - 10$) clusters and the equilibrium geometries of Ag_nCo ($n = 1 - 9$) clusters are illustrated in Table 1. The lowest energy structure of the AgCo dimer is found to favor de triplet spin multiplicity with a binding energy of 2.07 eV and Ag–Co bond length of 2.43 Å, larger than that of the Ag_2 dimer. In Table 2 the bond lengths of Ag_2 and Co_2 dimers are compared with recent reports, and have been found in fair agreement with experimental and theoretical results. Those results can give us an insight of the respective bond length of CoAg, which presented intermediate values between pure silver and cobalt dimers. The structure of Ag_2Co with $1\mu_B$ corresponds to a nearly equilateral triangle, while an open triangle with an angle of 70° which has $3\mu_B$ represents the ground state configuration. For Ag_3Co, the lowest energy structure was found to favor a planar rhombus for both LS and HS configurations ($\mu_T = 0$ or $2\mu_B$). For Ag_4Co clusters, the ground state geometry shows a similar structure conformation than the free Ag_5 cluster where Co is bonded by four Ag atoms. Trends to favor planar structures continue up to Ag_4Co where Co can be treated as substitutional impurity on pure Ag_n clusters. The lowest energy structures for Ag_5Co have slightly irregularities in the bond distances differing to the perfect C_{5v} pentagonal pyramid for $\mu_T = 1$ or $3\mu_B$. The lowest energy structure of Ag_5Co is the same compared with the obtained by Janssens et al., based on DFT calculations using the hybrid B3LYP functional

Table 1
Lowest energy structures of Ag_{n+1} and Ag_nCo (n = 1–9) clusters. For each cluster the total magnetic moment (in μ_B), symmetry point group, and bond distances (in Å) are given. The gray and blue spheres represent Ag and Co atom, respectively.

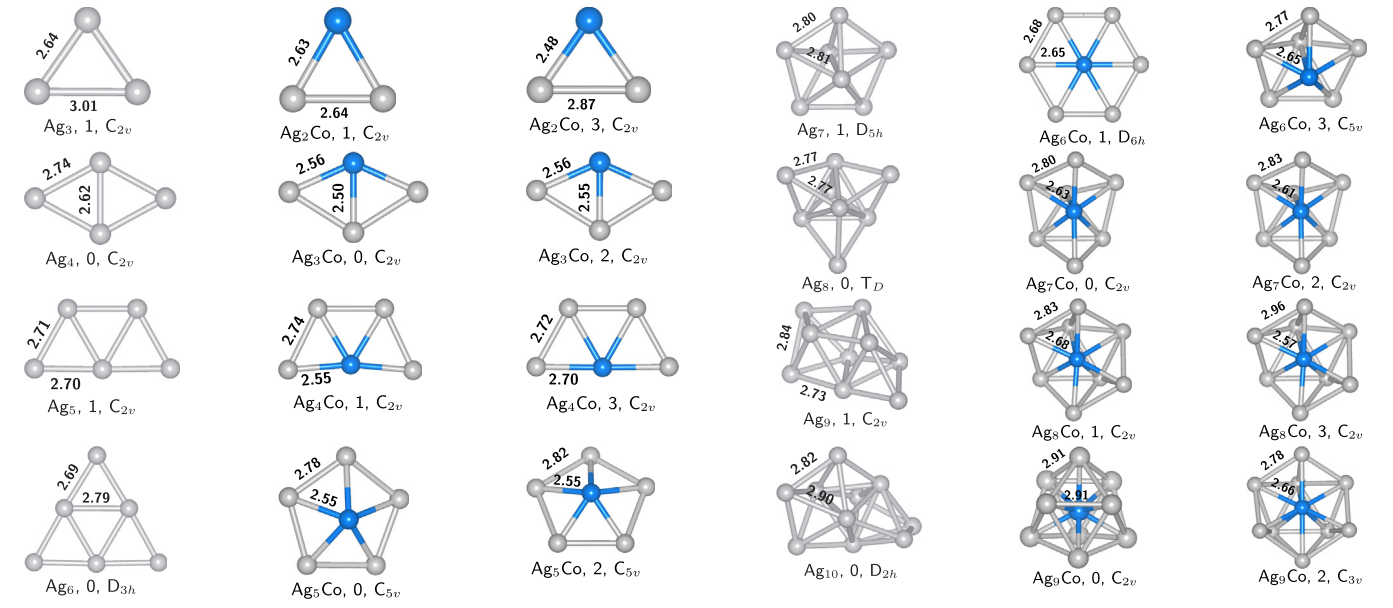

[41]. For Ag_6Co a D_{6h} planar symmetric geometry is found to represent the ground state structure having $\mu_T = 1\mu_B$. In the HS ($\mu_T = 3\mu_B$), Ag_6Co adopts a C_{5v} PBP structure. For Ag_nCo clusters from $n = 7$ onwards, with the addition of Ag atoms, the growth of Ag_nCo clusters continues with trends to form the icosahedral structure I_h. Interestingly for Ag_9Co, the Co impurity falls into the center of a Ag_n cage structure. This structure can be described as a C_{2v} distorted square antiprism capped by one Ag atom on the top, with an encapsulated Co atom. This result suggests that from $n = 9$ onwards, Ag_nCo clusters can adopt interesting structures which can differ from the icosahedral motif. In particular, the Co dimer has a bond distance 1.96 Å, which is shorter than in the Ag dimer of 2.58 Å, based in our approximation. By this, the geometries of Ag_nCo which have $n \leqslant 5$ clusters typically adopt the C_{2v} symmetry due to the Co–Ag bond-length reduction which is in practice 4% on average lower than the Ag–Ag one. The total average bond distances of the Ag_n and doped Ag_nCo clusters are presented in Fig. 1. The bond distances of the Ag_nCo clusters for both LS and HS are quite similar except for Ag_6Co and Ag_9Co by a change in the cluster structure. This behavior will be explained depending on the magnetic orderings between Co and the Ag_n host.

3.2. Energetic properties

Silver and cobalt atoms are immiscible at the bulk limit. The superficial energy of Ag is lower than Co, therefore it goes to the surface to minimize the total energy of the clusters [47]. In our results the single Co impurity increases the electronic stability of the Ag_n clusters decreasing the total ground state energy in both the LS ($\mu_T = 0$ or $1\mu_B$) and HS ($\mu_T = 2$ or $3\mu_B$) configurations. The stability of Ag_n and Ag_nCo clusters were investigated by calculating the binding energy per atom (E_b), defined as

$$E_b = \frac{E_T[Ag_n]}{n} - E_T[Ag] \quad (1)$$

for the bare Ag_n clusters, and

$$E_b = (E_T[Ag_nCo] - nE_T[Ag] - E_T[Co])/(n+1), \quad (2)$$

for Ag_nCo clusters, where $E_T[Ag]$, $E_T[Co]$, $E_T[Ag_n]$ and $E_T[Ag_nCo]$ are the total energies of the bare Ag atom, the Co atom, the Ag_n cluster and the Ag_nCo doped cluster, respectively. Fig. 2 shows the atom binding energy of pure Ag_n and Ag_nCo clusters. For the bare Ag_n clusters, E_b gradually increases with the cluster size n rapidly up to $n \leqslant 8$ and then the size dependence become smooth at $n > 8$. The results of E_b suggest that the substitution of Ag by a Co atom

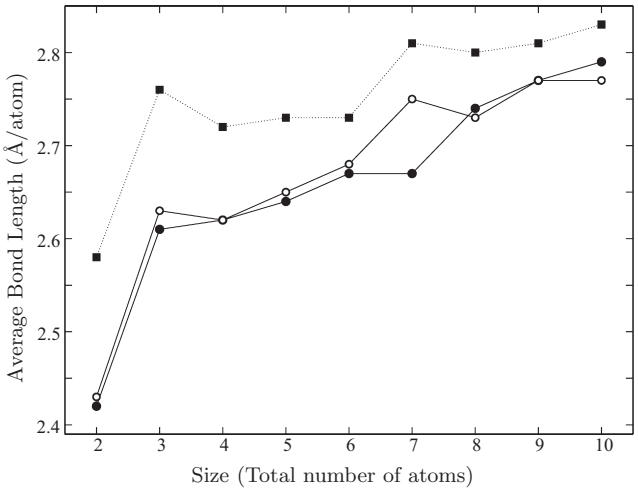

Fig. 1. Average bond distances of Ag_n (squares) and Ag_nCo clusters for the LS (solid circles) and HS (open circles) configurations of each cluster size.

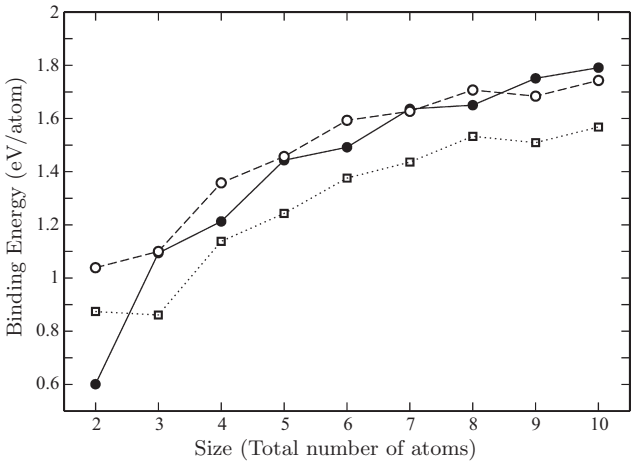

Fig. 2. Binding energies of Ag_n (squares) and Ag_nCo clusters for the LS (open circles) and HS (solid circles) configurations of each cluster size.

in Ag_n leads to improve the overall binding. The higher bond strength of Ag–Co over Ag–Ag indicates higher localization of valence electrons along the Ag–Co bond, by this, the Co impurity prevail in the highest coordinated site. This behavior can be extended to the nanoparticle region. For AgCo nanoparticles with enough Ag content, the formation of core–shell structures is possible [1]. For Ag_nCo clusters, larger values of the binding energy are found to increase as a function of the size with small oscillations for odd–even sizes depending on the number of valence electrons in the cluster. Unlike Ag_nCo clusters, Ag_n clusters show less oscillations in the binding energy curve. For odd sized Ag_nCo clusters the binding energy gap between the LS and HS is relatively small for Ag_nCo, suggesting that those clusters can have both magnetic moments $\mu_T = 1$ and $3\mu_B$, having similar stability. For even sized Ag_nCo clusters the HS (with $2\mu_B$) configuration is more stable, except for Ag_9Co. It is important to realize, that the highest E_b is found for Ag_9Co having a total magnetic moment of $0\mu_B$. We attributed such enhanced stability to a full 18-electron shell structure which is related to a magic number of itinerant electrons. The so-called magic numbers correspond to cluster sizes which completely fill electron shells. For Ag_n clusters they appear for n = 2, 8, 18, 20, and so on, in the size dependent intensity peaks observed in mass spectrometric investigations [48], which provide evidence of the enhanced stabilities with respect to their neighbors. From mass spectra analysis of Ag_nCo^+ clusters, an enhanced stability peak has been observed for the $Ag_{10}Co^+$ cationic cluster [20], provided that the Co impurity delocalize their valence 4s and 3d electrons, and each Ag atom contributes its one valence 5s electron (minus one because of the positive charge) what constitutes the 18-electrons complete shell. In the same manner, the theoretical stability of the neutral Ag_9Co cluster can be explained by the 18-electron rule. Similar cases have been reported previously for silicon doped clusters, e.g., for Si_9Co [10], $Si_{12}Cr$ [49], and $Si_{10}Fe$ [50], respectively. In order to clarify the stability with respect to the magnetic configurations, in Fig. 3 we show the relative isomer energy spectrum for Ag_nCo ($n = 2 - 9$) clusters (the LS and HS are presented by solid circles and crosses, respectively). In accordance with E_b, we also can observe from the isomer illustration (Fig. 3), that odd sized clusters favor the HS for the most stable isomers whereas for even sized clusters there are a crosslinking effect over the spin configurations, however, from the heptamer onwards, trends to adopt the non-magnetic or LS configurations for Ag_nCo clusters are observed.

In Table 3 the results of E_b are shown including the average Co–Ag bond length. For n = 2,4 and 6 of Ag_nCo clusters, E_b shows

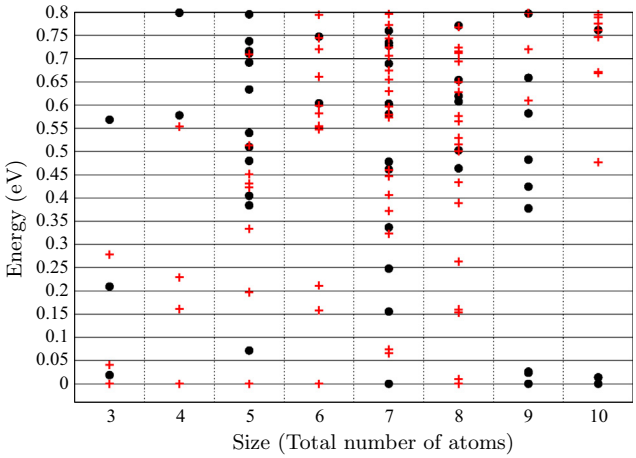

Fig. 3. Relative energy of Ag_nCo clusters isomers for the LS (circles) and HS (crosses).

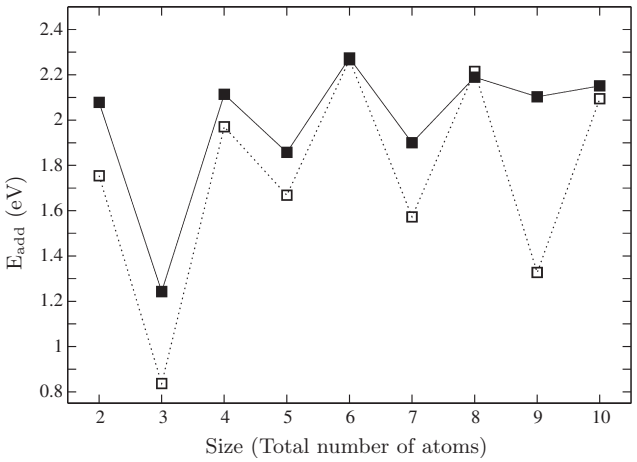

Fig. 4. Energy gain upon the addition of an extra Ag atom of Ag_n (open squares) and Ag_nCo clusters (closed squares) for the most stable clusters as a function of size.

Table 2
Calculated equilibrium bond length for Ag_2, Co_2 and CoAg dimers in their FM or NM (non-magnetic) states.

Dimer	State	Method	Functional	Bond length (Å)
Ag_2	NM	LCAO[a]	VWN	2.50
	NM	BO molecular-dynamics[b]	PBE	2.63
	NM	LCAO[c]	PBE	2.61
	NM	Exp[d]		2.53
	NM	This work	PBE	2.58
Co_2	FM	PAW[e]	PBE	1.96
	FM	PAW[f]	PW91	1.97
	FM	This work	PBE	1.96
	FM	PAW[g]	PBE	1.96
	FM	CRENBL-ECP[h]	BLYP	2.13
		Exp[i]		2.31
AgCo	FM	This work	PBE	2.43
	NM	This work	PBE	2.42

[a] Ref. [38].
[b] Ref. [36].
[c] Ref. [37].
[d] Ref. [35].
[e] Ref. [46].
[f] Ref. [42].
[g] Ref. [43].
[h] Ref. [44].
[i] Ref. [45].

Table 3
Numerical values of the binding energy E_b and average Co–Ag bond distances of Ag_nCo clusters as a function of size.

Ag_nCo	n								
	1	2	3	4	5	6	7	8	9
E_b (eV/atom)									
LS (0, 1 μ_B)	0.60	1.09	1.21	1.44	1.49	1.63	1.65	1.75	1.79
HS (2, 3 μ_B)	1.03	1.10	1.35	1.45	1.59	1.62	1.70	1.68	1.74
Co–Ag (Å)									
LS (0, 1 μ_B)	2.42	2.48	2.53	2.57	2.55	2.66	2.60	2.60	2.63
HS (2, 3 μ_B)	2.43	2.63	2.54	2.59	2.55	2.65	2.61	2.67	2.66

close values for both the LS and HS, these energies are a strong indication that many isomers are probably observed in experiments. A different way to present the size dependence of cluster energies is the energy gain E_{add} uppon the addition of an extra Ag atom $Ag_n \rightarrow Ag_{n-1} + Ag$, which is presented in Fig. 4. There is and even–odd oscillation in cluster energies which is more obvious than for E_b. The addition of a dopant Co atom on Ag_n clusters increase the value of E_{add}, which is consistent with our previous observations.

3.3. Magnetic properties and charge profiles

The incorporation of Co impurity on Ag_n increases or decreases the value of the magnetic excitation energy, defined as $\Delta E_m = E(HS) - E(LS)$ with respect to the HS configuration, taking into account the total energy of the cluster. A negative value of ΔE_m occur whether HS corresponds to the ground state. Fig. 5 shows the value of ΔE_m as a function of the size. We observe an oscillatory behavior with significant excitation energies (0.4 eV $< |\Delta E_m| <$ 1.0 eV) for even sizes corresponding to the singlet–triplet gap ($E = T - S$) which favor the HS state for $n \leqslant 8$. For the odd sizes the values of ΔE_m are very small ($\Delta E_m < 0.1$ eV) suggesting that the $\mu_T = 3$ or $1\mu_B$ moments are energetically close to each other. It is important to note that for Ag_9Co the triplet-singlet energy gap is found to be positive (going from $\mu_T = 0\mu_B$ to $\mu_T = 2\mu_B$), identifying the electronic state as a singlet.

To explore in a better detail the magnetic stability, we carried out a Bader analysis for the local charge and magnetic moments of Ag_nCo clusters. The Bader charge analysis showed that the Co impurity in general transfers charge to the Ag_n host. This amount of transfer v_{Co} is not too small and it increases monotonically and saturates at a value of about 0.4 (e). The value of the charge transfer to Ag_n depends slightly on the average Co–Ag bond distance, as it is shown in Fig. 6

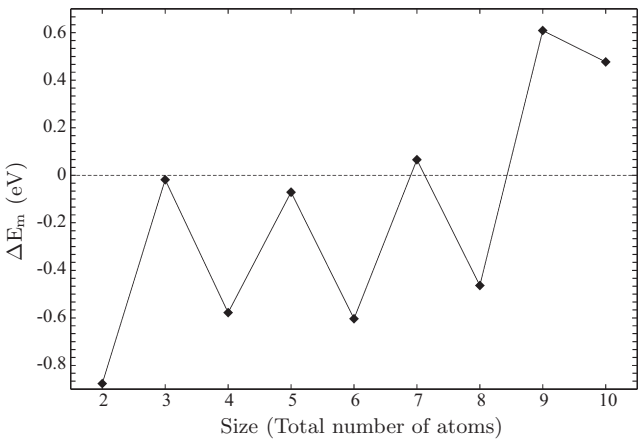

Fig. 5. Magnetic excitation energy of Ag_nCo clusters as a function of size.

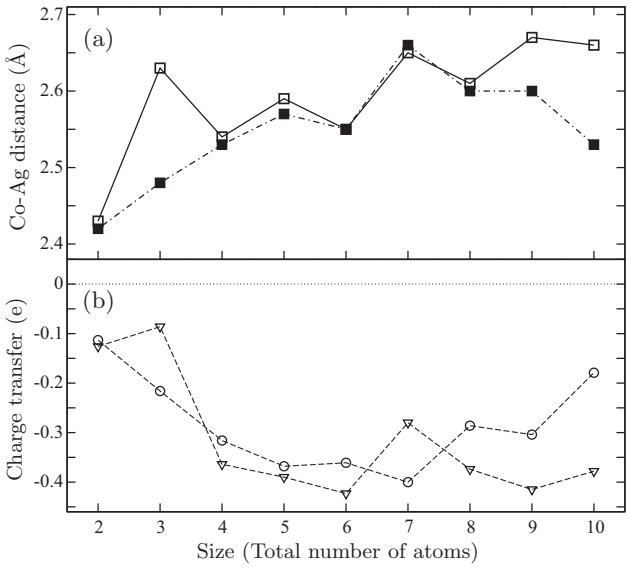

Fig. 6. (a) Average Ag–Co bond distance for Ag_nCo clusters for the LS (filled squares) and HS (open squares). (b) Total charge transfer from Co to the Ag_n host on Ag_nCo clusters as a function of size for the LS (circles) and HS (triangles).

The local magnetic moments μ_i of Ag_nCo clusters are plotted in Fig. 7 as a function of the total number of atoms present in the cluster. In this Figure the Co impurity $\mu(Co)$ (solid lines) and Ag_n host $\mu(Ag_n)$ magnetic moments (dashed lines) are presented for LS (circles) and HS (triangles) configurations. In order to clarify the magnetic orderings between the impurity and the metal host, for simplicity we discuss the magnetic orderings by odd and even values of the size separately. It has been shown by the binding energy gaps that odd sized clusters correspond to states energetically equivalent or fluxional states. The Bader analysis shows that these states correspond to weak FM orderings between Co and the Ag atoms for the HS, where $\mu_T = 3\mu_B$, while for the LS ($\mu_T = 1$) the clusters have AFM orderings. For even sized clusters, the binding energy is favored for the HS ($\mu_T = 2\mu_B$) having weak AFM orderings between Co and the Ag atoms. In addition, the ground state of the Ag_nCo clusters correspond to magnetic configurations where the Co impurity develops a saturated magnetic moment ($\mu(Co) \geqslant 2\mu_B$) having different magnetic orderings with the Ag_n host. These orderings are of AFM character for the odd sized clusters and FM for the even cases. Due the diamagnetic character of silver and small values of his local magnetic moments ($\mu_i \leqslant 0.1\mu_B$), fluctuations in the magnetic orderings can occur for odd sized Ag_nCo clusters. In order to illustrate the magnetic orderings for small Ag_nCo clusters, the isosurfaces of the local spin polarization for Ag_3Co and Ag_4Co in the LS and HS are shown in Table 4. We can observe saturated magnetic moments of Co in all cases except for Ag_3Co in the LS, where the magnetic moment of Co is reduced, reducing its stability. For larger Ag_nCo clusters, we found that the singlet spin multiplicity $\mu_T = 0\mu_B$ is adopted only by the endohedral Ag_9Co cluster. In this particular case, the Co impurity loses his magnetic degree of freedom in accordance to the Bader analysis.

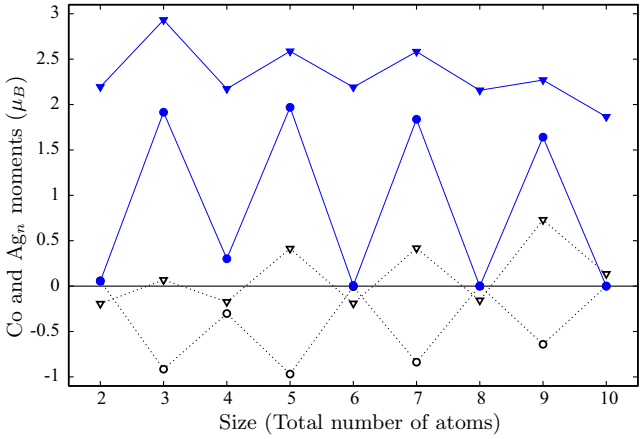

Fig. 7. Local magnetic moments of Ag_nCo clusters as a function of size, for Co (solid lines) and the Ag_n host (dashed lines) in the HS (circles) and LS (triangles) configurations.

Table 4
Isosurface of the local spin polarization for the most stable structures of Ag_3Co and Ag_4Co clusters for the LS (top) and HS (bottom) configurations.

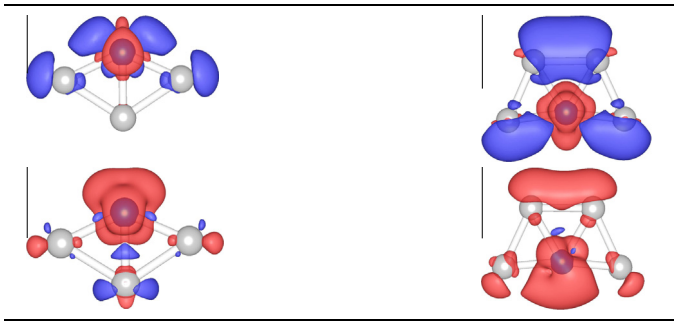

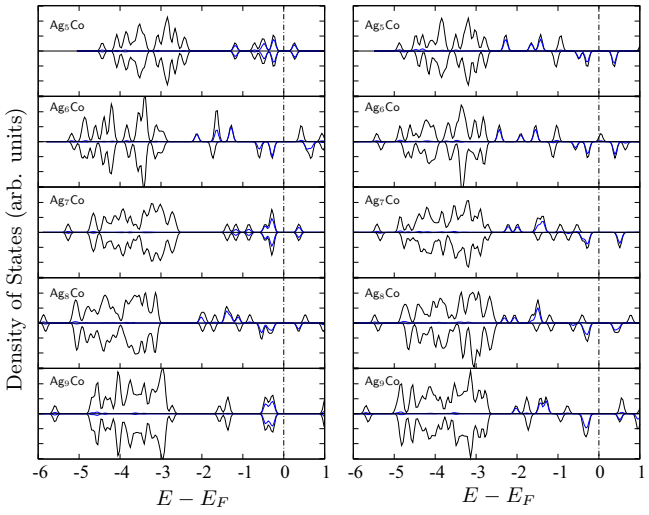

Fig. 8. Spin-polarized density of states of Ag_nCo clusters ($n = 5 - 9$) for both LS (left) and HS (right) spin configurations. The total DOS of Ag_nCo clusters and Co impurity curves are presented in black and blue lines, respectively. A Gaussian broadening of $\sigma = 0.2$ was used for the DOS curve. The Fermi energy (vertical dashed line) was taken as the zero of energy.

3.4. Electronic structure

The density-of-states (DOS) plot provides a complementary information to identify changes in the electronic and geometrical structure of the clusters [46]. In Fig. 8 we present the total spin-polarized DOS curve for a set of Ag_nCo clusters including the Co impurity total DOS, going in size from 5 to 9 atoms in the LS and HS configurations. The analysis of the Co DOS curve showed that the Co magnetic moment comes mainly from the *d* open shell. These states are not completely filled, therefore the Co preserves

an open shell electronic configuration in accordance with its valence electronic configuration. In the right side corresponding to the HS configuration, significant splittings of the majority and minority states of Co near the Fermi level E_F are observed, thus the Co atom is primarily responsible for the cluster magnetic behavior, which is consistent with the Bader analysis. On the other hand, for LS configurations, the even sized Ag_nCo clusters also present splittings of the majority and minority states near E_F in accordance with the AF orderings performed by Co and the Ag_n host. The special cases occur for odd sized clusters, for example, for Ag_5Co, Ag_7Co and Ag_9Co clusters in the LS configuration, no splitting of the majority and minority states are present in the DOS curve, corroborating that the Co moment is quenched; however, only for Ag_9Co the singlet state is energetically favorable suggesting a closed-shell electronic structure.

4. Summary and conclusions

In this work, the magnetic and structural properties of Ag_n clusters doped with a single Co impurity were investigated. We carried out density functional theory calculations for Ag_nCo $(n = 1 - 9)$ clusters considering a number of initial structures and magnetic configurations and found that the Co impurity can dramatically change the structural growth of Ag_nCo clusters for a specific size. For the ground state structures of the Ag_nCo clusters, the Co impurity falls into the most coordinated site. The lowest energy structures for Ag_nCo $(n \leqslant 4)$ clusters are planar while from $n = 5$ onwards, 3*D* structures are observed with an icosahedral growth motif except for the Ag_9Co endohedral cluster. In accordance with the binding energy, odd sized Ag_nCo clusters are energetically favored for the HS $(\mu_T = 2\mu_B)$, whereas for even sized clusters, the LS and HS $(\mu_T = 1$ or $3\mu_B)$ have a similar stability since the Co atom and the Ag_n host can adopt weak FM and AFM orderings preserving the local magnetic moment of Co $(\mu(Co) \geqslant 2\mu_B)$, however, from $n = 7$ onwards, trends to adopt the non-magnetic configurations for Ag_nCo clusters are observed. For Ag_9Co the Ag_n host quenches the magnetic moment of the encapsulated Co atom. Although the magnetic impurity leads to a reduction of the total magnetic moment of Ag_nCo clusters which is unfavorable for magnetic applications, it may be exploited for other applications such as catalysis.

Acknowledgements

This research is supported by the CONACYT Grant No. 221811. The computational resources were provided by the Centro Nacional de Super Computo CNS (San Luis Potosí, México).

Appendix A. Supplementary material

Supplementary data associated with this article can be found, in the online version, at http://dx.doi.org/10.1016/j.comptc.2015.05.009.

References

[1] J. Bansmann, S. Baker, C. Binns, J. Blackman, J.-P. Bucher, J. Dorantes-Dávila, V. Dupuis, L. Favre, D. Kechrakos, A. Kleibert, K.-H. Meiwes-Broer, G. Pastor, A. Perez, O. Toulemonde, K. Trohidou, J. Tuaillon, Y. Xie, Magnetic and structural properties of isolated and assembled clusters, Surf. Sci. Rep. 56 (2005) 189–275.
[2] A.W. Castleman, S.N. Khanna, Clusters, superatoms, and building blocks of new materials, J. Phys. Chem. C 113 (2009) 2664–2675.
[3] M.J. Moses, J.C. Fettinger, B.W. Eichhorn, Interpenetrating As20 fullerene and Ni12 icosahedra in the Onion-Skin $[As@Ni12@As20]^{3-}$ ion, Science 300 (2003) 778–780.
[4] Q. Sun, Q. Wang, P. Jena, B.K. Rao, Y. Kawazoe, Stabilization of Si_{60} cage structure, Phys. Rev. Lett. 90 (2003) 135503.
[5] Y. Li, N.M. Tam, P. Claes, A.P. Woodham, J.T. Lyon, V.T. Ngan, M.T. Nguyen, P. Lievens, A. Fielicke, E. Janssens, Structure assignment, electronic properties, and magnetism quenching of endohedrally doped neutral silicon clusters, Si_nCo $(n = 10 - 12)$, J. Phys. Chem. A 118 (2014) 8198–8203.
[6] V. Kumar, Design of Nanomaterials by Computer Simulations, CRC Press, 2010. pp. 1–23.
[7] P. Claes, V.T. Ngan, M. Haertelt, J.T. Lyon, A. Fielicke, M.T. Nguyen, P. Lievens, E. Janssens, The structures of neutral transition metal doped silicon clusters, Si_nX (n = 6–9; X = V, Mn), J. Chem. Phys. 138 (2013) 194301.
[8] V. Kumar, Y. Kawazoe, Metal-encapsulated fullerenelike and cubic caged clusters of silicon, Phys. Rev. Lett. 87 (2001) 045503.
[9] Y. Li, J.T. Lyon, A.P. Woodham, A. Fielicke, E. Janssens, The geometric structure of silver-doped silicon clusters, ChemPhysChem 15 (2014) 328–336.
[10] L. Ma, J. Zhao, J. Wang, Q. Lu, L. Zhu, G. Wang, Structure and electronic properties of cobalt atoms encapsulated in Si_n $(n = 1 - 13)$ clusters, Chem. Phys. Lett. 411 (2005) 279–284.
[11] P. Claes, E. Janssens, V.T. Ngan, P. Gruene, J.T. Lyon, D.J. Harding, A. Fielicke, M.T. Nguyen, P. Lievens, Structural identification of caged vanadium doped silicon clusters, Phys. Rev. Lett. 107 (2011) 173401.
[12] H. Kawamura, V. Kumar, Y. Kawazoe, Growth, magic behavior, and electronic and vibrational properties of Cr-doped Si clusters, Phys. Rev. B 70 (2004) 245433.
[13] L. Ma, J. Zhao, J. Wang, B. Wang, Q. Lu, G. Wang, Growth behavior and magnetic properties of Si_nFe $(n = 2 - 14)$ clusters, Phys. Rev. B 73 (2006) 125439.
[14] Q. Jing, F.-Y. Tian, Y.-X. Wang, No quenching of magnetic moment for the Ge_nCo $(n = 1 - 13)$ clusters: first-principles calculations, J. Chem. Phys. 128 (2008) 124319.
[15] W.-J. Zhao, Y.-X. Wang, Geometries, stabilities, and electronic properties of $(n = 9 - 16)$ clusters: density-functional theory investigations, Chem. Phys. 352 (2008) 291–296.
[16] L.-M. Wang, S. Bulusu, W. Huang, R. Pal, L.-S. Wang, X.C. Zeng, Doping the golden cage Au16- with Si, Ge, and Sn, J. Am. Chem. Soc. 129 (2007) 15136–15137.
[17] N.M. Tam, H.T. Pham, L.V. Duong, M.P. Pham-Ho, M.T. Nguyen, Fullerene-like boron clusters stabilized by an endohedrally doped iron atom: B_nFe with n = 14, 16, 18 and 20, Phys. Chem. Chem. Phys. 17 (2015) 3000–3003.
[18] T.M. Bernhardt, L.D. Socaciu-Siebert, J. Hagen, L. Wöste, Size and composition dependence in CO oxidation reaction on small free gold, silver, and binary silvergold cluster anions, Appl. Catal. A: Gen. 291 (2005) 170–178.
[19] L. Peyser, A. Vinson, A. Bartko, R. Dickson, Photoactivated fluorescence from individual silver nanoclusters, Science 291 (2001) 103–106.
[20] E. Janssens, S. Neukermans, H.M.T. Nguyen, M.T. Nguyen, P. Lievens, Quenching of the magnetic moment of a transition metal dopant in silver clusters, Phys. Rev. Lett. 94 (2005) 113401.
[21] E. Janssens, X.J. Hou, M.T. Nguyen, P. Lievens, The geometric, The geometric, electronic, and magnetic properties of Ag_5X+ (X=Sc, Ti, V, Cr, Mn, Fe, Co, and Ni) clusters, J. Chem. Phys. 124 (2006) 184319.
[22] S. Li, R.V. Zee, W. Weltner Jr., K. Raghavachari, Si_3–Si_7. Experimental and theoretical infrared spectra, Chem. Phys. Lett. 243 (1995) 275–280.
[23] H. Hiura, T. Miyazaki, T. Kanayama, Formation of metal-encapsulating Si cage clusters, Phys. Rev. Lett. 86 (2001) 1733–1736.
[24] P. Hohenberg, W. Kohn, Inhomogeneous electron gas, Phys. Rev. 136 (1964) B864–B871.
[25] W. Kohn, L.J. Sham, Self-consistent equations including exchange and correlation effects, Phys. Rev. 140 (1965) A1133–A1138.
[26] J.P. Perdew, K. Burke, M. Ernzerhof, Generalized gradient approximation made simple, Phys. Rev. Lett. 78 (1997) 1396.
[27] P.E. Blöchl, Projector augmented-wave method, Phys. Rev. B 50 (1994) 17953–17979.
[28] G. Kresse, J. Hafner, Ab initio molecular dynamics for liquid metals, Phys. Rev. B 47 (1993) 558–561.
[29] G. Kresse, J. Furthmüller, Efficient iterative schemes for ab initio total-energy calculations using a plane-wave basis set, Phys. Rev. B 54 (1996) 11169–11186.
[30] R.P. Feynman, Forces in molecules, Phys. Rev. 56 (1939) 340–343.
[31] G. Henkelman, A. Arnaldsson, H. Jónsson, A fast and robust algorithm for Bader decomposition of charge density, Comput. Mater. Sci. 36 (2006) 354–360.
[32] R.F.W. Bader, Atoms in Molecules, John Wiley and Sons, Ltd, 2002.
[33] Y. Wang, T.F. George, D.M. Lindsay, A.C. Beri, The Hückel model for small metal clusters. I. Geometry, stability, and relationship to graph theory, J. Chem. Phys. 86 (1987) 3493–3499.
[34] J.J. Moré, Z. Wu, Global continuation for distance geometry problems, SIAM J. Optim. 7 (1997) 814–836.
[35] B. Simard, P.A. Hackett, A.M. James, P.R. Langridge-Smith, The bond length of silver dimer, Chem. Phys. Lett. 186 (1991) 415–422.
[36] H. Häkkinen, M. Moseler, U. Landman, Bonding in Cu, Ag, and Au clusters: relativistic effects, trends, and surprises, Phys. Rev. Lett. 89 (2002) 033401.
[37] H. Grönbeck, A. Hellman, A. Gavrin, Structural, energetic, and vibrational properties of NO_x adsorption on Ag_n, $n = 1 - 8$, J. Phys. Chem. A 111 (2007) 6062–6067.
[38] R. Fournier, Theoretical study of the structure of silver clusters, J. Chem. Phys. 115 (2001) 2165–2177.
[39] C. Majumder, S.K. Kulshreshtha, Structural and electronic properties of Au_n $(n = 2 - 10)$ clusters and their interactions with single S atoms: ab initio molecular dynamics simulations, Phys. Rev. B 73 (2006) 155427.

[40] H.M. Lee, M. Ge, B.R. Sahu, P. Tarakeshwar, K.S. Kim, Geometrical and electronic structures of gold, silver, and goldsilver binary clusters: origins of ductility of gold and goldsilver alloy formation, J. Phys. Chem. B 107 (2003) 9994–10005.
[41] X.-J. Hou, E. Janssens, P. Lievens, M.T. Nguyen, Theoretical study of the geometric and electronic structure of neutral and anionic doped silver clusters, $Ag_5X^{0,-}$ with X = Sc, Ti, V, Cr, Mn, Fe, Co, and Ni, Chem. Phys. 330 (2006) 365–379.
[42] E.G. Moroni, G. Kresse, J. Hafner, J. Furthmüller, Ultrasoft pseudopotentials applied to magnetic Fe, Co, and Ni: from atoms to solids, Phys. Rev. B 56 (1997) 15629–15646.
[43] S. Datta, M. Kabir, S. Ganguly, B. Sanyal, T. Saha-Dasgupta, A. Mookerjee, Structure, bonding, and magnetism of cobalt clusters from first-principles calculations, Phys. Rev. B 76 (2007) 014429.
[44] A. Sebetci, Cobalt clusters (Co_n, $n = 0 \leqslant 6$) and their anions, Chem. Phys. 354 (2008) 196–201.
[45] A. Kant, B. Strauss, Dissociation energies of diatomic molecules of the transition elements. ii. Titanium, chromium, manganese, and cobalt, J. Chem. Phys. 41 (1964) 3806–3808.
[46] C.D. Dong, X.G. Gong, Magnetism enhanced layer-like structure of small cobalt clusters, Phys. Rev. B 78 (2008) 020409.
[47] L. Favre, S. Stanescu, V. Dupuis, E. Bernstein, T. Epicier, P. Mélinon, A. Perez, Nanostructured thin films from mixed magnetic CoAg clusters, Appl. Surf. Sci. 226 (2004) 265–270.
[48] E. Janssens, S. Neukermans, X. Wang, N. Veldeman, R.E. Silverans, P. Lievens, Stability patterns of transition metal doped silver clusters: dopant- and size-dependent electron delocalization, Euro. Phys. J.D 34 (2005) 23–27.
[49] S.N. Khanna, B.K. Rao, P. Jena, Magic numbers in metallo-inorganic clusters: chromium encapsulated in silicon cages, Phys. Rev. Lett. 89 (2002) 016803.
[50] S. Khanna, B. Rao, P. Jena, S. Nayak, Stability and magnetic properties of iron atoms encapsulated in Si clusters, Chem. Phys. Lett. 373 (2003) 433–438.